

ALBEDO CONTRAST DETERMINATION IN THE NEIGHBOURHOOD OF MARTIAN DUST DEVIL TRACKS. T. Statella¹, P. Pina² and E. A. Silva³, Instituto Federal de Educação, Ciência e Tecnologia de Mato Grosso – IFMT, 95 Zulmira Canavarro 780025-200, Cuiabá, Brazil (thiago.statella@cba.ifmt.edu.br), ²CERENA, Instituto Superior Técnico - IST, Av. Rovisco Pais 1049-001, Lisboa, Portugal (ppina@ist.utl.pt), ³Universidade Estadual Paulista, Faculdade de Ciências e Tecnologia – FCT, 305 Roberto Simonsen 19060-900, Presidente Prudente, Brazil (erivaldo@fct.unesp.br).

Introduction: Dust devil tracks are albedo patterns on planetary surfaces that result from the removal of particles by the presence of a dust devil to expose an underlying surface with a different albedo. On Mars, dust devil tracks densities were shown to change with the time of the year, suggesting that dust devil activity also depends on season [1-2]. Those albedo features tend to fade with time, which is attributed to the deposition of dust [3-4]. Albedo measurements can shed light on the nature of the surface materials and can be used to derive the thermal inertia and to evaluate the heat balance of Mars. We introduce and test here an automated methodology to compute the albedo contrast between dust devil tracks and their surroundings which can be used to indirectly infer the relative depth of the dust coat on large image datasets of Mars.

Method: The sequence developed to compute the albedo contrast on images is based on 3 main steps:

1. *Segmentation of the tracks:* this task gives a binary image of the tracks as output through a method mainly based on mathematical morphology operators [5] capable of achieving high performances (average of 92% of correct detections in MOC/NA and HiRISE images).
2. *Determination of track widths:* This value permits to establish the dimension of the neighborhood to analyse in the albedo computation. The mean width of the tracks in each scene is computed by a morphological granulometric analysis, which gives information about sizes of the connected components (the tracks) in the image. The dilation of the detected tracks permits creating a mask of the neighboring regions (Figure 1).
3. *Computation of the albedo contrast:* Once defined the neighborhood of the tracks, the radiance factor (I/F) for the pixels belonging to tracks and for those pixels belonging to their neighboring regions is computed. I/F is defined as the ratio of the bidirectional reflectance of a surface to that of a normally illuminated perfectly diffuse surface:

$$I / F = I / \pi F \quad (1)$$

where I is the measured scene radiance in $W / m^2 / \mu m / sr$, and πF is the solar irradiance at the top of the Martian atmosphere in $W / m^2 / \mu m$ at the time of the observation and through a particular band. The radiance factor I/F can be further converted into an estimated Lambert Albedo A_L through division by the cosine of the solar incidence angle for each pixel.

This measure allows for direct comparison between scenes taken at different times of day once it reduces illumination effects [6]. Two keywords in the Planetary Data System provide a mechanism to translate the DN integer value of the HiRISE image to I/F : the scaling factor SF and $Offset$ values. The equation is as follows:

$$I / F = (DN \times SF) + Offset \quad (2)$$

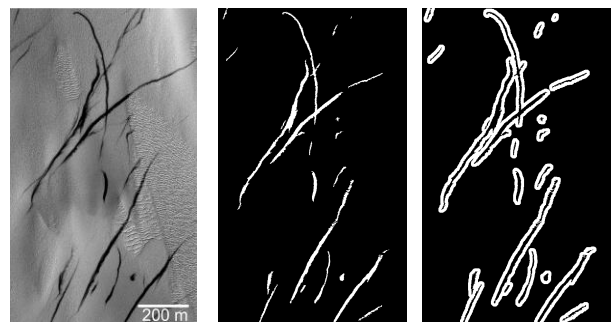


Figure 1. Sequence to compute relative albedo contrast: (a) HiRISE image PSP_006163_1345; (b) automated tracks detection; (c) mask of neighboring regions [Image credits: NASA/JPL/University of Arizona].

Experimental: The search for images containing tracks was driven by evidences that dust devils are more likely to occur in the southern hemisphere during spring and summer [3,4,7]. The selected 41 HiRISE images depict regions in the Mars Chart quadrangles of Aeolis (MC23), Argyre (MC26), Noachis (MC27), Hellas (MC28) and Eridania (MC29). Their spatial resolution was either 0.25 m (about 90%) or 0.50 m. Therefore, the solar longitude (L_s) of the scenes varied between 180° and 360° in these latitudes. The initial dataset resulted in practice into 107 images that were trimmed to its regions of interest (some images contained two or more of these regions), so irrelevant information such as large areas with no tracks was discarded. We calculated the albedo of the tracks and their neighboring regions for all 107 images. The global results for each MC, also discriminated by spring and summer seasons, are shown in Table 1, which contains the mean albedo for the tracks, for the neighbor regions (Nr) and the mean albedo contrast between these two features.

Table 1. Albedo computation results on five MC quadrangles.

Region	Season	Nb. Images	Mean Track Albedo	Mean Nr Albedo	Mean Albedo Contrast
Argyre	Spring	2	0.1992	0.2056	0.0064
	Summer	53	0.1747	0.2041	0.0294
	Total	55	0.1757	0.2042	0.0285
Aeolis	Spring	1	0.2211	0.2408	0.0197
	Summer	-	-	-	-
	Total	1	0.2211	0.2408	0.0197
Eridania	Spring	10	0.1524	0.1739	0.0215
	Summer	9	0.1593	0.1960	0.0367
	Total	19	0.1557	0.1843	0.0286
Noachis	Spring	6	0.1568	0.1716	0.0148
	Summer	13	0.1501	0.1806	0.0305
	Total	19	0.1528	0.1778	0.0250
Hellas	Spring	-	-	-	-
	Summer	16	0.1776	0.2069	0.0293
	Total	16	0.1776	0.2069	0.0293

There are some overall differences between regions (when the total albedo is considered), which is much more evident when spring and summer are separately considered, not only between the seasons of the same region but also between the same season between distinct regions.

Eridania quadrangle showed a mean albedo contrast of 2.86% considering spring and summer. Hellas quadrangle showed the highest contrast and Aeolis showed the lowest one, both only with summer images. When data from spring and summer are considered, the contrast in summer is higher, as expected [1-2]. The highest mean albedo contrast in summer is found in Eridania (3.67%) and the lowest one in Hellas. Argyre quadrangle showed the higher albedo contrast variation between spring and summer, which was 2.30%. This high albedo contrast was probably due to the deposition of dust during autumn and winter seasons in Argyre [3-4].

In [2] and [8] it was raised the hypothesis that the contrast between albedo tracks and their surroundings, which varies from region to region, is related to the depth of the dust layer. For instance, dust devil tracks are darker in Noachis and brighter in Aeolis, which suggests that the dust devils in Aeolis were not big enough to excavate the surface and expose the substrate. Assuming that [2] and [8] are right, then the regions in Hellas quadrangle have a thinner layer of dust coverage than the others. On the other hand, Aeolis and Noachis have little thicker dust coat. In general, the mean track albedo was lower than the 20% related in [6]. The exception is Aeolis region which showed a mean track albedo of 22%.

The local analysis provided by our method permits to quantitatively analyse in detail the same region in a multitemporal basis. Russell crater (54.9°S, 347.6° W)

is an interesting site for dust devil tracks observation: a total of 32 images between 2007 and 2012 were processed to compute the mean albedo of the exact same region of interest (a pair of examples is provided in Figure 2).

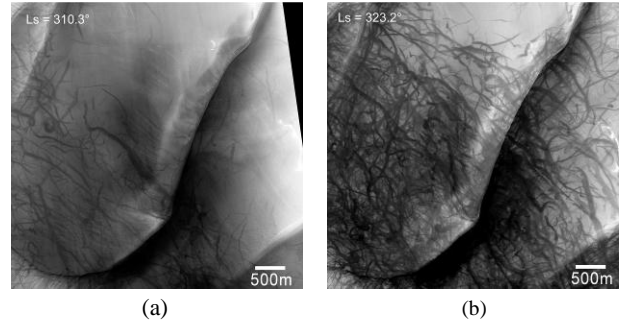


Figure 2. Examples of changes in dust devil tracks in Russell crater on HiRISE images: (a) PSP_005238_1255, 08/Sept/2007; (b) PSP_005528_1255, 01/Oct/2007 [Image credits: NASA/JPL/University of Arizona].

The results obtained for the whole sequence are shown in Figure 3, where circles stand for images where no dust devil tracks were observed and triangles stand for images showing those tracks. The main conclusion is that, in general, higher albedos were found during the winter seasons when most of the images have no tracks. The detailed conclusions to be withdrawn from this sequence will be presented somewhere else.

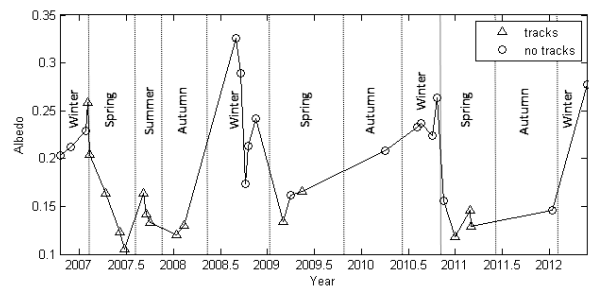


Figure 3. Temporal analysis of the albedo in a region of Russell crater (the vertical dotted lines are used to group images belonging to the same season and do not represent, therefore, the whole length of seasons).

Acknowledgment: We thank CAPES agency for financial support.

References: [1] Thomas et al. (2003) *Icarus* 162, 242-258. [2] Whelley et al. (2006) *JGR* 111, E10003. [3] Malin M. et al. (2001) *JGR* 106, E10. [4] Balme M. et al. (2003) *Rev. Geophys.* 44, RG3003. [5] Statella et al. (2012) *PSS* 70, 46-58. [6] Bell et al. (2006) *JGR*, 111, E02S03. [7] Örmö and Komatsu (2003) *JGR*, 108, E6, 5059. [8] Verba et al., *JGR*, 115, E09002.